

Degree of ionization in antiprotonic noble gases

R. Bacher, P. Blüm, D. Gotta,* K. Heitlinger, and M. Schneider

*Institut für Kernphysik und Institut für Experimentelle Kernphysik der Universität,
Kernforschungszentrum Karlsruhe G.m.b.H., Postfach 3640, D-7500 Karlsruhe 1, Federal Republic of Germany*

J. Missimer and L. M. Simons

Paul Scherrer Institut,† CH-5234 Villigen, Switzerland

K. Elsener

European Organization for Nuclear Research (CERN), CH-1211 Geneva 23, Switzerland

(Received 23 May 1988)

The ionization of antiprotonic noble-gas atoms due to formation and Auger deexcitation was investigated. The experiment was performed at low target pressures ($p \leq 50$ hPa) in order to prevent electron refilling from neighboring atoms. For this reason, the cyclotron trap was used. This device is designed to stop as many particles as possible in a small stop volume at even low gas pressure. The degree of ionization was determined in antiprotonic neon, argon, and krypton by means of measuring yields of circular radiative transitions at relatively high principal quantum numbers. X rays were observed between 1.6 and 21.0 keV using a Si(Li) detector. Complete ionization was found in all three cases.

I. INTRODUCTION

Experiments dealing with exotic atoms extract information from measurements of x-ray transition energies as well as from measurements of x-ray transition intensities. Both quantities are strongly influenced by the status of the electron shell. For example, the precision of measurements to determine QED corrections or to extract the mass of the exotic particle is presently limited by the uncertainty in the number of electrons. This renders the accurate calculation of electron screening corrections¹⁻³ and the reconstruction of the measured line shape³ difficult. Another example is the measurement of a parity violation effect in atomic systems due to the neutral weak current interaction, which is manifested in the mixing of the $2s$ and $2p$ states in light muonic atoms. Its study is based on the observation of the radiative $M1$ transition ($\gamma M1: 2s \rightarrow 1s$).⁴⁻⁶ This task is only feasible if the quenching of the $2s$ state due to nonradiative decay is hindered. For example, in μNe , the Auger transition ($eE1: 2s \rightarrow 2p$), accompanied by the ejection of an L -shell electron, must be suppressed. This requires the ionization of all but the two K -shell electrons.⁷

Discussion of the ionization of exotic atoms due to formation and nonradiative deexcitation dates back to the fundamental work of Fermi and Teller.⁸ In 1953, de Borde⁹ investigated theoretically the ionization due to Auger deexcitation and the dependence of the Auger rates on the electron shell configuration. Later, this investigation was extended mainly by Vogel,¹⁰⁻¹³ who studied static screening and atomic aftereffects.

Leon and Seki¹⁴ discussed dynamic electron screening, i.e., the participation of supposedly passive electrons in a transition of an exotic atom. This effect becomes important if exotic and electronic transition energies are degenerate.

Several authors^{1,15-18} dealt with electronic K x-ray satellites originating from electron shell rearrangement processes caused by the deexcitation of the exotic atom. The satellite energies reflect the electron shell configuration.

Whereas electronic x-rays were investigated experimentally in only a few cases, measurements of intensities and energies of exotic x-rays (Auger electron lines were observed in only one case¹⁹) yielded a wealth of information about the occupation of the electron shell. For example, partial depletion of the L and M shell was found by Hartmann *et al.*²⁰ in solid-state materials with low atomic number Z . In high- Z elements, a high degree of ionization could be excluded.²⁰⁻²³ Recently, in muonic argon at low pressure, Jacot-Guillarmod *et al.*²⁴ achieved the best fit to their data by assuming complete ionization. This result confirms an earlier proposal of the authors of the present paper.²⁵

In these cases, the observed x rays were emitted at the end of the electromagnetic cascade. The electron shell configuration at earlier stages was determined via numerical model calculations. However for solids, liquids, or high-pressure gases, the most investigated materials, this procedure is ambiguous due to electron refilling from neighboring atoms.

In this paper, we report on a measurement determining the degree of ionization of exotic (in this case antiprotonic) noble-gas atoms that is not based on model-dependent cascade calculations.

The use of antiprotonic atoms has some advantages compared to other atoms containing lighter exotic particles. First, the number of cascade steps below the K shell scales roughly according to $\sqrt{m/m_e}$ (m denotes the reduced mass of the exotic particle, m_e the reduced electron mass), yielding more numerous measurable transitions. Second, corresponding x-ray energies are higher,

which implies less self-absorption. Third, antiprotons can be stopped more easily since the advent of low-energy antiproton beams. This facilitates experiments at very low target pressures.

II. THEORETICAL BACKGROUND

At the beginning of this section, a short survey of typical attributes of exotic atoms is given. The idea of our measurement is based on speculations of Fermi and Teller⁸ in 1947. The method described in the present paper is restricted to isolated atoms. The section ends with a presentation of a formula due to Ferrell.²⁶ This formula is used in order to support quantitatively our interpretation of the measured x-ray spectra.

An antiprotonic atom commonly loses one electron during the capture of an antiproton. The kinetic energy of the incoming particle prior to capture amounts to $O(10 \text{ eV})$, which is of the same order of magnitude as the atomic ionization potential.²⁷⁻³¹ After that, the atom is in a loosely bound atomic or molecular state from which the deexcitation starts. By the time the antiproton is localized within the K shell, i.e., $n = \sqrt{m/m_e} \leq 43$ (n denotes the principal quantum number), the antiprotonic cascade proceeds between the levels of a hydrogenlike

atom. At present, only this section of the cascade can be investigated experimentally. In atoms with $Z \geq 3$, the cascade is characterized by two competing processes:^{32,33} Auger transitions, progressing via the ejection of an electron, are dominant in the upper and middle part of the cascade, provided that electrons are available to be ejected. In contrast, radiative transitions prevail in the lower part, independent of the current electron population. The upper limit of this lower cascade section increases slowly with atomic number, from $n \approx 7$ for neon to $n \approx 11$ for krypton.

In contrast to Auger transitions, radiative transitions prefer the maximum energy difference possible. Therefore, all transitions starting from states with different principal (n) but the same orbital (l) quantum numbers tend to populate the same final circular level. A circular level is characterized by an orbital quantum number $l = n - 1$. It can only deexcite via a ($|\Delta n| = 1$) dipole transition into the following circular state. This feature of the radiative deexcitation process leads to an accumulation of antiprotons in the circular levels and to a predominating deexcitation via a circular cascade.

For two reasons, a high degree of ionization can be expected due to the Auger effect. First, an antiproton has enough energy to eject all but the two K -shell electrons

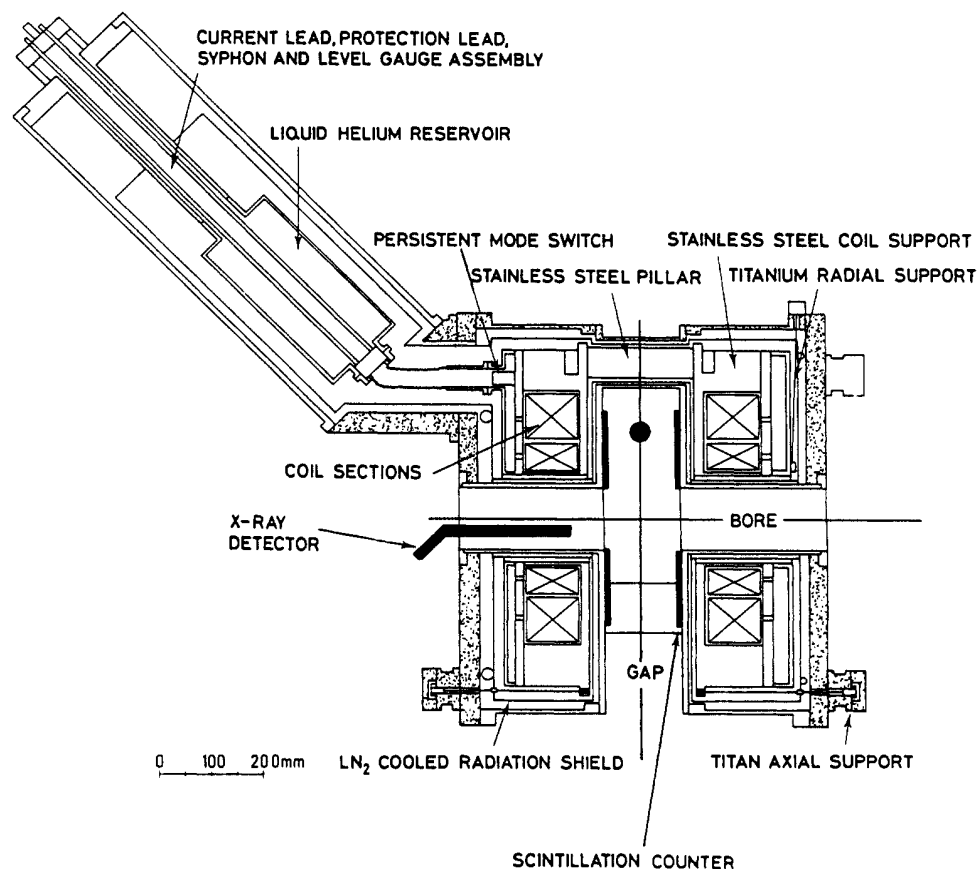


FIG. 1. Experimental setup. The cross section of the cyclotron trap is shown. The target chamber is placed within the gap and the axial bores of the magnet. The positions of the x-ray detector [Si(Li)] and the scintillation counters, which observe pions resulting from antiproton-nucleon annihilation, are indicated. The detector crystal is located within the tip of the detector's end cap. The dot denotes the beam injection point into the weak-focusing cyclotron field.

by the time it reaches the state $n = 40, 34,$ and 27 for antiprotonic neon, argon, and krypton, respectively. Second, the highly excited energy levels of an antiprotonic atom are almost degenerate and the electrons in the upper shells (L, M, \dots) can be described as an electron gas. Therefore it can be assumed that electrons are always available for Auger deexcitation in this range.

As a result of progressive ionization of the atom due to the Auger effect the minimum ionization energy increases. As suggested first by Fermi and Teller⁸ and later on by de Borde⁹ and by Griffith *et al.*,³⁴ the fast Auger-predominated cascade via circular or nearly circular orbits is interrupted if the transition energy becomes smaller than the minimum ionization energy. Radiative transitions are still possible at this stage of the cascade but proceed slowly. For example, in krypton, the radiative lifetime of the circular ($n = 27$)-state amounts to $O(10^{-13}$ s). This is 2 orders of magnitude longer than the corresponding Auger lifetime. Therefore, the further cascade is delayed until a substantial part of the ionic charge is neutralized due to electron transfer via collisions with neighboring atoms, diminishing the minimum ionization energy again.

To avoid electron transfer, the antiprotonic atoms must be isolated. For this reason, a gas target can be used. If the target pressure is low enough, the electron refilling proceeds slower than the competing radiative transition. The electron transfer probability λ_{trans} is given by

$$\lambda_{\text{trans}} = \sigma_{\text{trans}} \nu p. \quad (1)$$

The atomic recoil velocity ν can be deduced from spectral flux density measurements³⁰ of the incoming particles prior to capture and is $O(10^3$ m/s). The transfer cross section σ_{trans} ranges from $O(10^{-19}$ m²) for neon to $O(10^{-18}$ m²) in the case of krypton according to the successful semiclassical model described in the references.³⁵⁻³⁷ Considering a cascade, in which the first and slowest radiative transition starts from a state with a principal quantum number as estimated above ($n = 40, 34,$ and 27 for neon, argon, and krypton, respectively) lasting $O(10^{-10}$ s) to $O(10^{-13}$ s) for the considered cases, a target pressure p less than approximately 100 hPa is sufficient to prevent electron refilling.

Under these conditions the cascade proceeds mainly via a ladder of slow radiative ($|\Delta n| = 1$) dipole transitions between circular levels until the transition energy becomes large enough to eject electrons again. Then the cascade continues via nonradiative transitions, provided that the Auger transition width (Γ_{Aug}) is still much larger than the radiative one (Γ_{rad}). This assumption can be checked using an analytic approximation formula for electric dipole transitions due to Ferrell.²⁶ This formula turns out to be sufficient, and the use of a complex cascade program to be unnecessary, due to the simplicity of the circular cascade

$$\frac{\Gamma_{\text{Aug}}(\omega)}{\Gamma_{\text{rad}}(\omega)} = \frac{1}{(Z-1)^2} \frac{\sigma_{\text{photo}}^{(Z-1)}(\omega)}{\sigma_T}. \quad (2)$$

$\sigma_{\text{photo}}^{(Z-1)}$ denotes the photoelectric cross section for an atom with nuclear charge $Z-1$. It scales according to

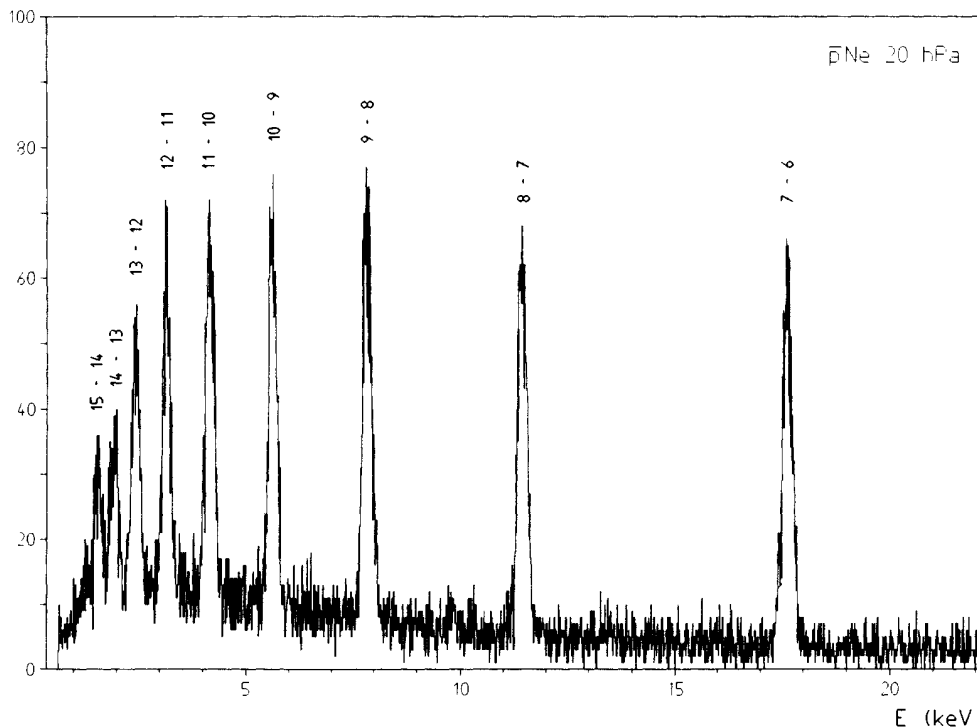


FIG. 2. Spectrum of antiprotonic neon measured at a target pressure of 20 hPa. The ordinate is the unnormalized number of counts.

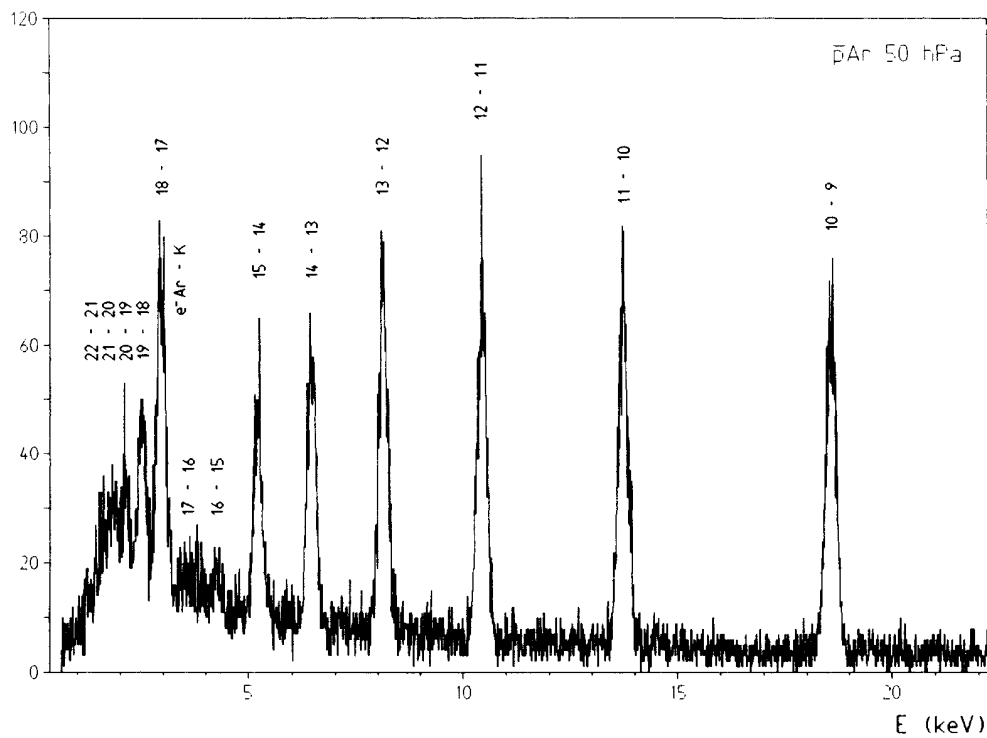


FIG. 3. Spectrum of antiprotonic argon measured at a target pressure of 50 hPa. The ordinate is the unnormalized number of counts.

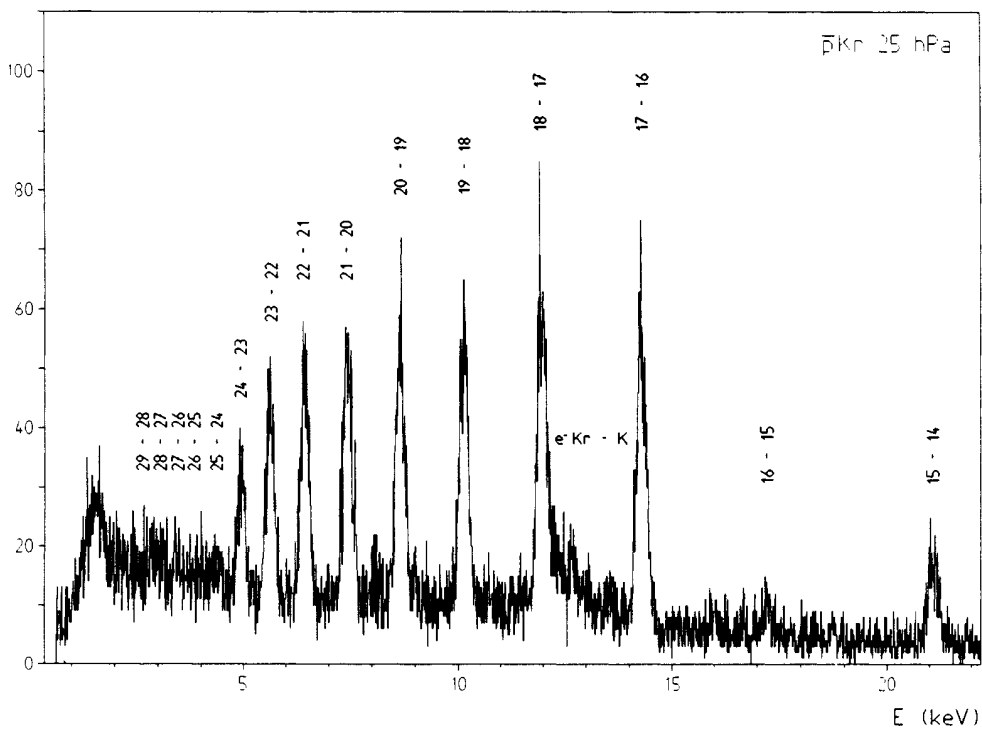


FIG. 4. Spectrum of antiprotonic krypton measured at a target pressure of 25 hPa. The ordinate is the unnormalized number of counts.

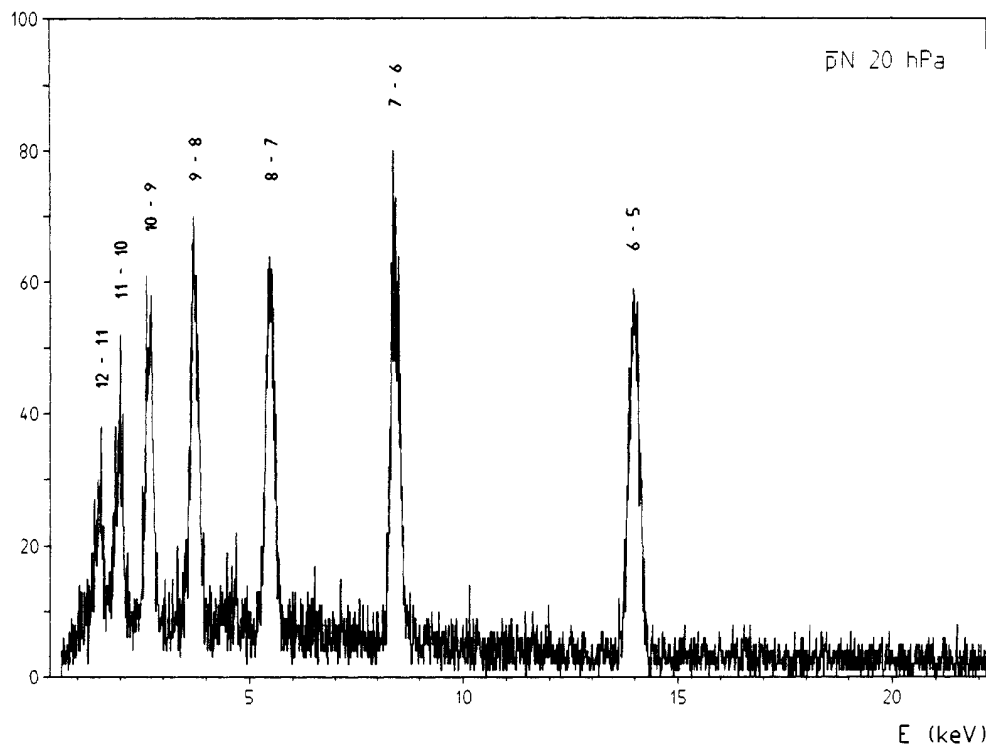


FIG. 5. Spectrum of antiprotonic nitrogen measured at a target pressure of 20 hPa. The ordinate is the unnormalized number of counts.

the electron occupation number. σ_T designates the Thomson scattering cross section and ω the transition frequency. Therefore by observation of radiative transitions during the Auger-dominated part of the cascade the electron shell occupation can be deduced experimentally.

III. EXPERIMENTAL SETUP AND DATA

The experiment was performed at the Low Energy Antiproton Ring (LEAR) facility at CERN. The setup is shown in Fig. 1. X rays from the antiprotonic noble gases neon, argon, and krypton were measured at energies less than about 20 keV at low target pressure ($p \leq 50$ hPa). Figures 2–4 show the raw spectra.

The task of stopping as many antiprotons as possible at low gas pressure, on the one hand, and in a small stop volume, on the other, was achieved using the cyclotron trap.³⁸ The incoming particles pass an injection moderator and enter a weak-focusing cyclotron field. After that, they lose their remaining energy due to ionization of target gas atoms. Thus the antiprotons are transported in spiral-shaped orbits from the periphery of the trap to a well-defined distribution at its center, where antiprotonic atoms are formed. The field is produced by a superconducting split-coil magnet, which permits maximum access to the stop region.

A small planar Si(Li)-semiconductor detector was used in order to observe the x rays originating from the formed atoms. Its characteristics are a 30-mm² active area, a 8- μ m-thick Be window and an energy resolution of 210 eV at 6.4 keV.

The problem of determining the relative detector efficiency was solved by comparing the antiprotonic neon spectrum (Fig. 2) with the corresponding nitrogen spectrum shown in Fig. 5. The antiprotonic cascades do not differ very much due to the nearly equal nuclear charges. The intensities of the lines 12-11, 11-10, and 10-9 should be almost identical. This is a general attribute of a radiative circular cascade resulting from the complete ionization of the atoms (see Sec. IV). This feature is evident in the neon spectrum. However, a strong but regular energy dependence of the line intensities is observed in the case of antiprotonic nitrogen, where the corresponding peak positions are shifted to smaller energies due to the reduced nuclear charge. Therefore, taking into account the trivial self-absorption correction, the energy dependence of the line intensities in both spectra reflects directly the relative in-beam detector efficiency. Its absolute value was fixed at 14.4 keV using a ⁵⁷Co standard source.

IV. RESULTS AND DISCUSSION

Table I presents all measured ($|\Delta n| = 1$) transition yields. Yield is defined as number of measured x rays per formed antiprotonic atom after correction for detector efficiency, solid angle and self-absorption. The number of formed antiprotonic atoms was determined via the observation of charged pions using scintillation counters. The pions result from the antiproton-nucleon annihilation during the electromagnetic cascade. These annihilation events are separated in time from annihilations during the deceleration of the antiprotons prior to capture.

TABLE I. Absolute yields of the measured circular radiative transitions ($|\Delta n| = 1$) of antiprotonic neon (20 hPa), argon (50 hPa), and krypton (25 hPa), respectively. The listed transition energies are calculated values (Ref. 39).

Transition $n_i \rightarrow n_f$	Ne		Ar		Kr	
	E (keV)	Y	E (keV)	Y	E (keV)	Y
29→28					2.766	0.423(0.201)
28→27					3.079	0.226(0.085)
27→26					3.441	0.171(0.059)
26→25					3.862	0.041(0.031)
25→24					4.355	0.109(0.029)
24→23					4.935	0.316(0.048)
23→22					5.623	0.453(0.063)
22→21			1.591	0.278(0.124)	6.446	0.447(0.059)
21→20			1.835	0.440(0.107)	7.437	0.450(0.059)
20→19			2.132	0.328(0.081)	8.641	0.457(0.058)
19→18			2.498	0.523(0.104)	10.122	0.463(0.058)
18→17			2.951	0.680(0.130)	11.960	0.475(0.059)
17→16			3.522	0.210(0.061)	14.272	0.474(0.059)
16→15			4.249	0.132(0.033)	17.221	0.061(0.011)
15→14	1.571	0.537(0.097)	5.195	0.511(0.089)	21.042	0.166(0.022)
14→13	1.948	0.492(0.077)	6.441	0.588(0.100)		
13→12	2.455	0.556(0.081)	8.120	0.624(0.104)		
12→11	3.155	0.589(0.076)	10.438	0.595(0.099)		
11→10	4.149	0.609(0.073)	13.729	0.593(0.098)		
10→9	5.609	0.573(0.064)	18.565	0.605(0.100)		
9→8	7.845	0.589(0.062)				
8→7	11.450	0.549(0.057)				
7→6	17.655	0.561(0.058)				

They can be identified clearly by measuring the time dependence of the annihilation products. In contrast to the yields of circular transitions, the yields of the measured ($|\Delta n| = 2$) transitions are small [$O(1\%)$] and not listed. The tabulated energies are calculated values using the computer code PBAR (Ref. 39) for transitions between lower levels ($n \leq 15$) and the Dirac-energy formula for a pointlike nucleus for transitions between higher levels.

A. Neon

In the case of antiprotonic neon (Fig. 6), a series of lines is observed. The lines belong to a nearly circular cascade. Their absolute yields are almost identical and the mean value amounts to $\bar{Y} = 0.564(0.023)$. The missing yield reflects the still incomplete accumulation of antiprotons in the circular levels. As well as annihilating with nucleons during the cascade, the antiprotons populate the numerous inner states, which produce less intensive transitions ($|\Delta n| \gg 1$). These transitions cannot be observed by our x-ray detector due to their high energies. This statement is corroborated by cascade calculations. Complete ionization can be deduced from the observed spectrum. Our conclusion is based on two arguments.

First, according to Ferrell's formula the relative Auger-transition probability increases strongly with decreasing energy, from 50% at 13 keV to 95% at 5 keV, even if only one K -shell electron is present. Hence, all transitions below about 13 keV and above the K -edge energy should proceed preferably via the Auger effect, provided that the K shell is not depleted completely. Auger

deexcitation prevails also in the less probable case of a single $2s$ electron for $E \leq 6$ keV. In contrast, the observed radiative circular transitions in this energy range furnishes evidence for complete depletion of the electron shell.

Second, the displayed cascade section corresponds to a cascade time of about 10^{-11} s. This should be compared with the K -hole lifetime ranging from 10^{-15} s in the case of a complete shell to 10^{-13} s in the case of a single $2p$ -shell electron. Therefore provided that electrons are present in higher shells, they would immediately refill the vacant K shell. Auger transitions would be possible and a strong suppression of lines in the spectrum would result. This is not observed.

The transition yields (Table I) are equal within the experimental errors. The reason for this is twofold: First, the relative probability for radiative deexcitation amounts to 100% and is the same for all transitions, because no electrons are available to be ejected. Second, the populations of successive circular states do not differ very much [(1–2)%]. This small difference results from the large number of states in an antiprotonic atom; therefore, the individual contributions of inner transitions feeding the circular levels are smaller than in lighter exotic atoms.

B. Argon

The spectrum of antiprotonic argon (Fig. 7) shows a drastic reduction of yield in the lines 17-16 and 16-15. The reduction manifests the depletion of the K shell. The

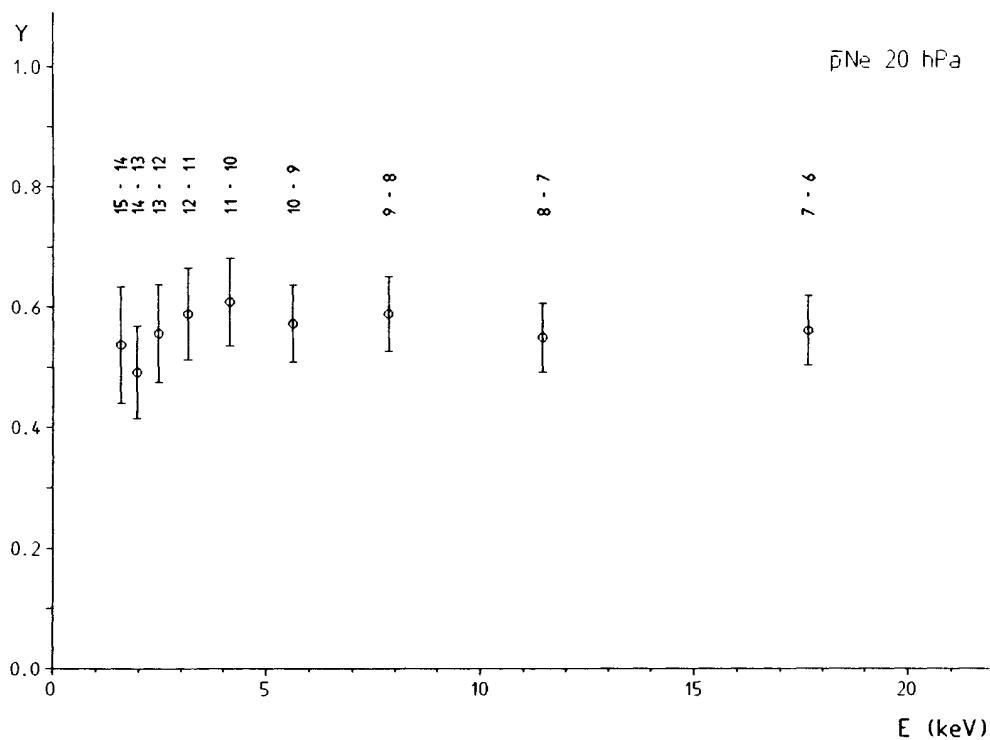


FIG. 6. Absolute yields of the measured radiative circular transitions ($|\Delta n| = 1$) of antiprotonic neon.

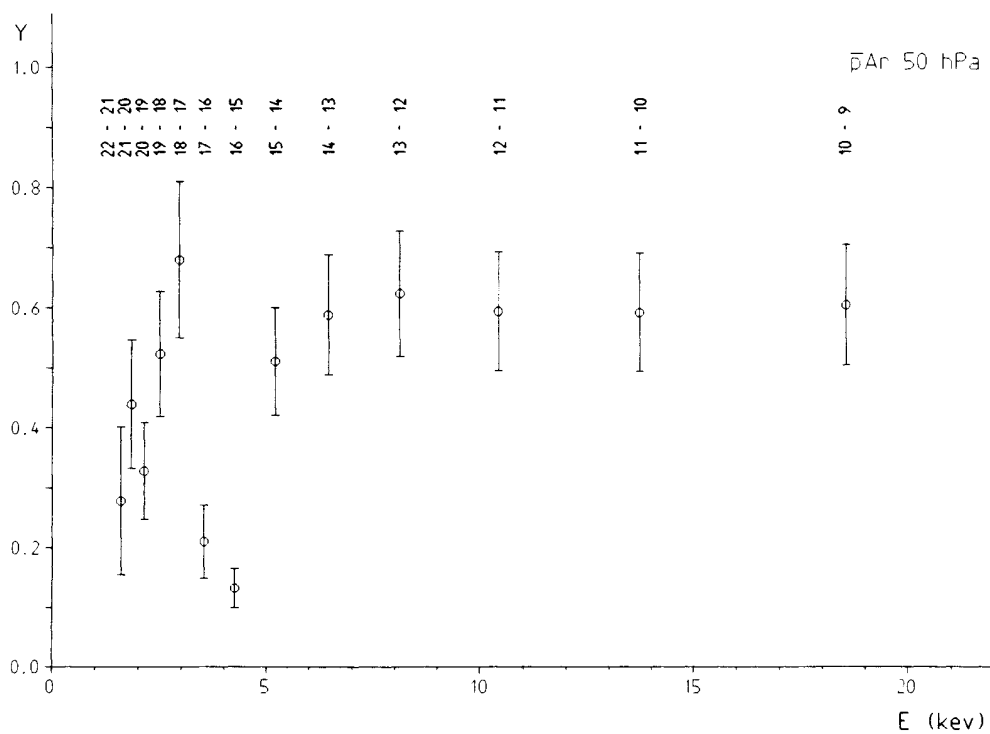


FIG. 7. Absolute yields of the measured radiative circular transitions ($|\Delta n| = 1$) of antiprotonic argon.

energies of the preceding transitions (from 22-21 to 18-17) are not sufficient to eject these electrons. However, the energy of the transition 17-16 exceeds the *K*-shell binding energy and the transition proceeds via the Auger effect. The conversion of exactly two lines, corresponding to the number of *K*-shell electrons, results.

For an argon atom with a complete electron shell, the transition 18-17 ($E_{18-17}=2.95$ keV) would be suppressed, because the ionization energy of a *K*-shell electron amounts to about 2.8 keV. On the other hand, in a system ionized of all but the two *K*-shell electrons, the removal of the remaining electrons requires 3.5 and 3.8 keV, while the energies of the transitions 17-16 and 16-15 amount to 3.52 and 4.25 keV, respectively. Therefore, they proceed via the Auger effect in accordance with the observed spectrum. All binding energies of partially ionized atoms are taken from the Refs. 40 or 41.

The yields of the suppressed lines amount to 21% and 13% (Table I), respectively, in contradiction to Ferrell's formula predicting almost complete suppression [$< O(1\%)$]. This shows that the *K* shell is already partially depleted by the same amount [$O(10\%)$] as indicated by the two line yields via ($|\Delta n| \geq 2$) transitions, before depletion due to circular transitions is possible. In addition, the arguments given for neon concerning *K*-hole refilling due to possible electrons in higher shells are also valid. The cascade segment between $n=15$ and 10 proceeds in 10^{-12} s. However, electron refilling from higher shells would take place within 10^{-14} s, even if only one *2p* electron would stay in the shell, and the suppression of lines would result. Therefore complete ionization has been established in antiprotonic argon.

C. Krypton

Compared to neon and argon, the energies of corresponding transitions in krypton are shifted to higher values due to the larger nuclear charge. For this reason, the spectrum of antiprotonic krypton (Fig. 8) shows an earlier stage of the cascade which includes both the depletion of the *L* shell and the depletion of the *K* shell (via 16-15, 15-14). It can be concluded, that antiprotonic krypton is completely ionized due to Auger effect during its electromagnetic cascade.

L-shell depletion apparently begins with the transition 28-27 and is completed after the transition 24-23. Otherwise the almost identical yields (Table I) of the following circular lines (from 23-22 to 17-16) cannot be understood. Figure 9 shows the energy dependence of the relative radiative transition probability $\Gamma_{\text{rad}}/\Gamma_{\text{tot}}$ ($\Gamma_{\text{tot}}=\Gamma_{\text{Aug}}+\Gamma_{\text{rad}}$) for different electron shell configurations as predicted by Ferrell's formula. The curves are calculated for energies above the *L*-edge energy. Complete depletion of the *M* and *N* shell is supposed. The probability and also the line yield rise with increasing energy, provided that electrons are present in the *L* shell. A constant probability and nearly constant yields can be expected only in the case of a shell completely ionized of all but the two *K*-shell electrons. The ejection of the remaining *K*-shell electrons via ($|\Delta n|=1$) transitions is forbidden until the transition 17-16 inclusive due to energy conservation.

Surprisingly, the observed depletion of the *L* shell involves the suppression of only five lines, although the maximum *L*-shell population amounts to eight electrons. This means, that the *L* shell is depleted already partially via noncircular transitions. The result is an electron shell

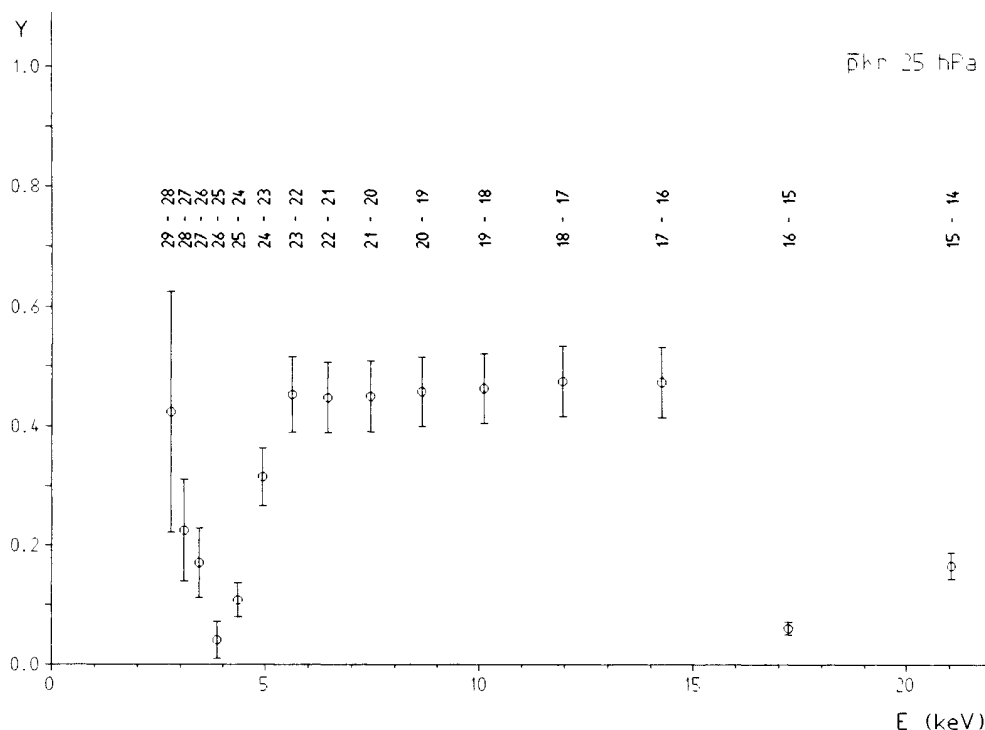


FIG. 8. Absolute yields of the measured radiative circular transitions ($|\Delta n| = 1$) of antiprotonic krypton.

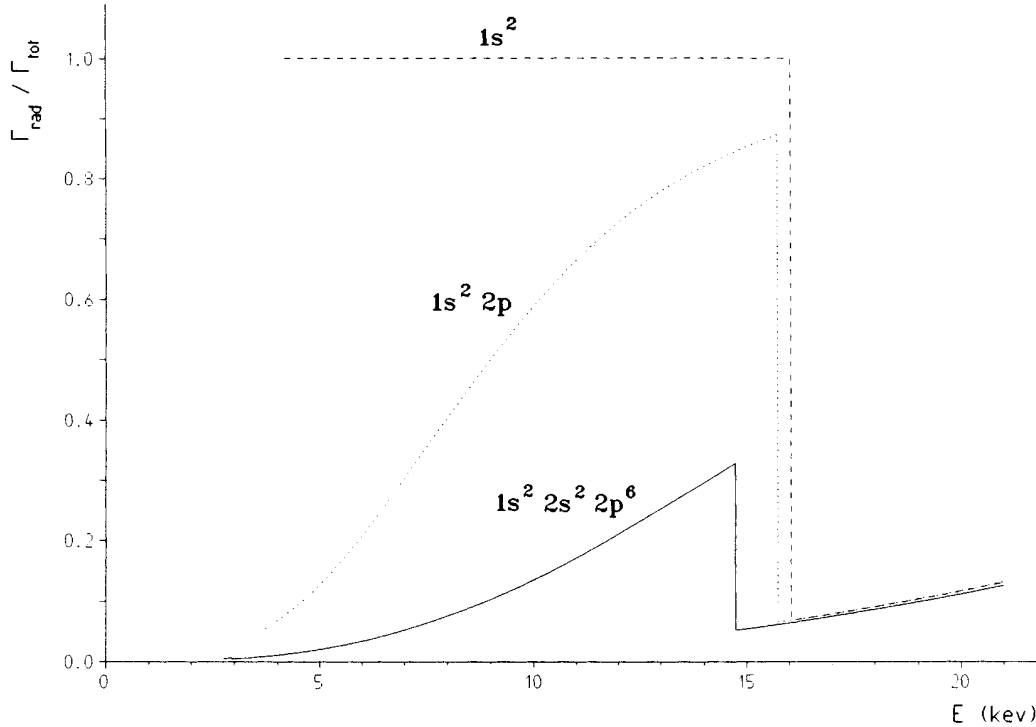


FIG. 9. Energy dependence of the relative transition probability $\Gamma_{\text{rad}}/\Gamma_{\text{tot}}$ ($\Gamma_{\text{tot}} = \Gamma_{\text{Aug}} + \Gamma_{\text{rad}}$) for different electron shell configurations in antiprotonic krypton as predicted by Ferrell's formula (Ref. 26). The curves are calculated for energies above the L -edge energy. Complete depletion of the M and N shell is supposed.

configuration ($1s^2 2s^2 2p^3$) by the time the antiproton reaches the ($n=28$) state. This configuration is indicated by three arguments: First, the line 29-28 ($E_{29-28} = 2.77$ keV) would be suppressed if the L shell were complete, because the L -shell ionization energy amounts to about 2.5 keV. Second, the initial configuration ($1s^2 2s^2 2p^3$) implies that an energy of about 3 keV is necessary to emit the next $2p$ electron. This is possible via the transition 28-27 ($E_{28-27} = 3.08$ keV), resulting in the observed suppression of the line yield. Third, the transitions 28-27 and 27-26 proceed via the Auger effect ejecting $2p$ electrons, because the $2s$ electrons are too tightly bound. The following transition 26-25 is able to emit both $2p$ and $2s$ electrons and the much more reduced yield of this transition can be explained by the larger rates for Auger-emission of $2s$ electrons. The depletion of the K -shell is effected via the almost nonradiative transitions 16-15 and 15-14 as already pointed out in the case of antiprotonic argon.

V. SUMMARY AND REMARKS

In this paper, we investigated the ionization of antiprotonic noble-gas atoms due to nonradiative deexcitation. Complete ionization is found in neon, argon, and krypton.

We have also measured x rays from antiprotonic xenon. The spectrum indicates a high degree of ionization. However, a final determination of the electron shell occupation is impossible using the Si(Li) detector available for the experiment.

There is evidence in all cases, that the ionization begins

with the loosely bound outer electrons and ends with the removal of the K -shell electrons. Thus, in this way a strong correlation exists during the cascade between the electron shell configuration, on the one hand, and the current antiprotonic state, on the other hand.

These observations open the possibility for precise spectroscopy of exotic atoms not affected by the influence of an unknown number of electrons.

(1) For example, a more accurate determination of the antiproton mass is feasible.

(2) The fine structure of light antiprotonic atoms, influenced by the anomalous magnetic moment, vacuum polarization, and recoil effects,⁴² can be investigated precisely.

(3) It seems possible to measure the polarization of the charge distribution of an antiproton⁴³ induced by the strong electric field of the atomic nucleus.

(4) Simple atomic systems with well-defined quantum numbers, consisting of a nucleus, an antiproton, and one electron, can be prepared almost at rest in order to determine QED corrections in one-electron atoms.⁴⁴

ACKNOWLEDGMENTS

The authors wish to thank Professor Dr. H. Pilkuhn for helpful suggestions and discussions. The efforts of the LEAR staff and the help of P. Gauss from the CERN Cryogenic Group are gratefully acknowledged. This work is part of the Ph.D. thesis of one of us (R.B.), University of Karlsruhe, 1987, Kernforschungszentrum Karlsruhe G.m.b.H. Report No. 4347 (unpublished).

- *Present address: Institut für Kernphysik, Kernforschungsanlage Jülich, Postfach 1913, D-5170 Jülich, Federal Republic of Germany.
- †Formerly Schweizerisches Institut für Nuklearforschung.
- ¹B. Fricke, *Lett. Nuovo Cimento* **2**, 859 (1969).
- ²H. J. Leisi, *Nucl. Phys.* **A335**, 3 (1980).
- ³B. Jeckelmann, T. Nakada, W. Beer, G. de Chambrier, O. Elsenhans, K. L. Giovanetti, P. F. A. Goudsmit, H. J. Leisi, A. Rüetschi, O. Piller, and W. Schwitz, *Phys. Rev. Lett.* **56**, 1444 (1986).
- ⁴G. Feinberg and M. Y. Chen, *Phys. Rev. D* **10**, 190 (1974).
- ⁵J. Bernabeu, T. E. O. Ericson, and C. Jarlskog, *Phys. Lett.* **50B**, 467 (1974).
- ⁶A. N. Moskalev, *Pis'ma Zh. Eksp. Teor. Fiz.* **19**, 394 (1974) [*JETP Lett.* **19**, 216 (1974)].
- ⁷J. Missimer and L. M. Simons, *Phys. Rep.* **118**, 179 (1985).
- ⁸E. Fermi and E. Teller, *Phys. Rev.* **72**, 399 (1947).
- ⁹A. H. de Borde, *Proc. Phys. Soc. London* **67**, 57 (1954).
- ¹⁰P. Vogel, *Phys. Rev. A* **7**, 63 (1973).
- ¹¹P. Vogel, *Phys. Rev. A* **8**, 2292 (1973).
- ¹²P. Vogel, *Phys. Rev. A* **22**, 1600 (1980).
- ¹³V. R. Akylas and P. Vogel, *Comput. Phys. Commun.* **15**, 291 (1978).
- ¹⁴M. Leon and R. Seki, *Nucl. Phys.* **A298**, 333 (1978).
- ¹⁵W. D. Fromm, Dz. Gansorig, T. Krogulski, H.-G. Ortlepp, S. M. Polikanov, B. M. Sabirov, U. Schmidt, R. Arlt, R. Engfer, and H. Schneuwly, *Phys. Lett.* **55B**, 377 (1975).
- ¹⁶P. Vogel, *Phys. Lett.* **58B**, 52 (1975).
- ¹⁷H. Schneuwly and P. Vogel, *Phys. Rev. A* **22**, 2081 (1980).
- ¹⁸K. Rashid and B. Fricke, *Z. Phys. A* **304**, 193 (1982).
- ¹⁹R. Calies, H. Daniel, F. J. Hartmann, and W. Neumann, *Phys. Lett.* **91A**, 441 (1982).
- ²⁰F. J. Hartmann, R. Bergmann, H. Daniel, H.-J. Pfeiffer, T. von Egidy, and W. Wilhelm, *Z. Phys. A* **305**, 189 (1982).
- ²¹J. L. Vuilleumier, W. Dey, R. Engfer, H. Schneuwly, H. K. Walter, and A. Zehnder, *Z. Phys. A* **278**, 109 (1976).
- ²²P. Vogel, A. Zehnder, A. L. Carter, M. S. Dixit, E. P. Hincks, D. Kessler, J. S. Wadden, C. K. Hargrove, R. J. McKee, H. Mes, and H. L. Anderson, *Phys. Rev. A* **15**, 76 (1977).
- ²³E. Bovet, F. Boehm, R. J. Powers, P. Vogel, K.-C. Wang, and R. Kunselman, *Phys. Lett.* **92B**, 87 (1980).
- ²⁴R. Jacot-Guillarmod, F. Bienz, M. Boschung, C. Piller, L. A. Schaller, L. Schellenberg, H. Schneuwly, and D. Siradovic, *Phys. Rev. A* **37**, 3795 (1988).
- ²⁵R. Bacher, D. Gotta, L. M. Simons, J. Missimer, and N. C. Mukhopadhyay, *Phys. Rev. Lett.* **54**, 2087 (1985).
- ²⁶R. A. Ferrell, *Phys. Rev. Lett.* **4**, 425 (1960).
- ²⁷P. Vogel, P. K. Haff, V. Akylas, and A. Winther, *Nucl. Phys.* **A254**, 445 (1975).
- ²⁸M. Leon and J. H. Miller, *Nucl. Phys.* **A282**, 461 (1977).
- ²⁹H. Schneuwly, V. I. Pokrovsky, and L. I. Ponomarev, *Nucl. Phys.* **A312**, 419 (1978).
- ³⁰G. Fottner, H. Daniel, P. Ehrhart, H. Hagn, F. J. Hartmann, E. Köhler, and W. Neumann, *Z. Phys. A* **304**, 333 (1982).
- ³¹T. von Egidy, D. H. Jakubassa-Amundsen, and F. J. Hartmann, *Phys. Rev. A* **29**, 455 (1984).
- ³²G. R. Burbidge and A. H. de Borde, *Phys. Rev.* **89**, 189 (1953).
- ³³Y. Eisenberg and D. Kessler, *Nuovo Cimento* **19**, 1195 (1961).
- ³⁴J. E. Griffith, P. K. Haff, and T. A. Tombrello, *Ann. Phys.* **87**, 1 (1974).
- ³⁵H. Ryufuku, K. Sasaki, and T. Watanabe, *Phys. Rev. A* **21**, 745 (1980).
- ³⁶R. Mann, F. Folkmann, and H. F. Beyer, *J. Phys. B* **14**, 1161 (1981).
- ³⁷A. Bárány, G. Astner, H. Cederquist, H. Danared, S. Hultdt, P. Hvelplund, A. Johnson, H. Knudsen, L. Liljeby, and K.-G. Rensfelt, *Nucl. Instrum. Methods B* **9**, 397 (1985).
- ³⁸L. M. Simons, in *Fundamental Symmetries*, Proceedings of the First Course of the International School of Physics "Ettore Majorana" International Science Series, Erice, Trapani, Sicily, Italy, 1986, edited by P. Bloch, P. Pavlopoulos, and R. Klapisch (Plenum, New York, 1987), Vol. 31, p. 89.
- ³⁹E. Borie and B. Jödicke, computer code PBAR (private communication).
- ⁴⁰T. A. Carlson, C. W. Nestor, N. Wassermann, and J. D. McDowell, *At. Data* **2**, 63 (1970).
- ⁴¹G. Zschornack, G. Musiol, and W. Wagner, *Akademie der Wissenschaften der DDR, Zentralinstitut für Kernforschung, Report No. 574*, 1986 (unpublished).
- ⁴²G. Bohnert, R. Decker, A. Hornberg, H. Pilkuhn, and H. G. Schlaile, *Z. Phys. D* **2**, 23 (1986).
- ⁴³T. E. O. Ericson and J. Hüfner, *Nucl. Phys.* **B47**, 205 (1972).
- ⁴⁴W. R. Johnson and G. Soff, *At. Data Nucl. Data Tables* **33**, 405 (1985).